Clean Qubits in Dirty Channels

Leo Thomas[a] **and Michael Hilke, Dr.**[a]

[a]Department of Physics, McGill University, 3600 Rue Université, Montréeal, QC, H3A 2T8, Canada

This manuscript was compiled on December 18, 2016

This project aims to study the coherence of entangled quantum bits (qubits) in the presence of static disorder. We first create a mathematical model for a well studied case: two qubits coupled by an electrostatic force, in order to confirm the accuracy of our method. We then apply this method to a system of two qubits entangled through a channel exhibiting various levels of static (time independent) disorder. We aim to establish a correlation between the disorder present in the channel and its effect on the preservation of the original qubits' states. We find that qubits entangled through channels exhibiting high levels of static disorder are more likely act as isolated, or decoupled, particles. We notice a sharp increase in decoupling probability as the disorder range exceeds the width of the channel. The effects of static disorder on qubit entanglement are not as well studied as those of dynamic (time dependent) disorder, for which correction schemes have been developed [1]. Studying entanglement in the presence of static disorder is a first step in developing techniques to mitigate these effects in experimental settings. These techniques will be useful to the development of technologies relying on quantum entanglement for faster and higher quality information transfer.

Quantum computation | Qubit entanglement | Quantum channel disorder

Quantum entanglement, which is crucial to the development of quantum computers and other related technologies, is, unfortunately, highly sensitive to disorder from both inside and outside of the entangled system. Disorder in quantum systems is almost always destructive and often leads to decoherence, or loss of information or energy from the system to its environment. In this case the wavefunctions of particles in the system may collapse, and these particles may fall back to classical states.

In quantum computers, quantum bits, or qubits, must be connected by a channel, such as a photon beam [2] or a fiber optic cable [3] in order to become entangled. In the ideal case this channel can be perfectly isolated from disorder, however this is not the case in practice. Disorder affecting a given system can come from time dependent sources (dynamic), such as background radiation and electromagnetic signals, or time independent (static) sources, such as impurities within the fiber optic cable connecting the two qubits, or simply impurities in the air through which the photon beam travels.

Quantum systems entangled in the presence of dynamic noise are well studied and have been found to exhibit high levels of decoherence. Accordingly, error correcting schemes have been developed to avoid these effects [1]. Entanglement in the presence of static disorder, on the other hand, is not as well studied, but equally problematic. Some quantum computers, for example, are required to be cooled to 20 millikelvins, in order to avoid decoherence due to environment temperature. [4].

The study of coherence in entangled quantum systems is consequential with the emergence of "quantum 2.0" technologies, technologies that use qubit entanglement to improve the precision of their measurements [5]. These technologies include improved atomic clocks, which can keep time with an order of magnitude more precision than the current leading clocks. These clocks use quantum entanglement to transmit information about the state of vibrating aluminum ion to a beryllium ion, whose light signals are easier to detect [6]. Electron microscopes and astronomic observation and measurement tools, such as satellites, are also among technologies which can be improved by quantum computing techniques [7].

This project creates mathematical models corresponding to two different quantum systems, and studies the dynamics of these systems as they are subjected to static disorder. The principal metric studied is the time evolution of their expectation values (probability of being found a given state). The first system is a well studied case: two qubits with an electrostatic coupling. This is used to confirm the accuracy of the method, which is then applied to our objective system: two qubit entangled through a channel with static disorder.

A consequential result of this investigation is the positive correlation between the amount of static disorder present within the quantum channel and its ability to preserve the original states of the entangled qubits, known as the channel's fidelity. As disorder in the channel increases, the original, unentangled, quit dynamics are recovered, a somewhat counter intuitive result. We also notice a sharp increase in fidelity occurring when the distribution range of disorder in the channel exceeds the channel's bandwith.

1. Results and Discussion

The metric we observe throughout this investigation is the qubit's expectation values, or the qubit's probability of being in a given state at a given time. Figure 1 shows the time evolution of expectation values of two qubits with different state energies (ε) and coupling energies (τ). We notice that

Significance Statement

Quantum computation offers an unprecedented increase in the efficiency of solving a large class of problems, including ones previously through unfeasible to perform on a classical computer. Integer factorization of two large primes, the foundation of public-private key cryptography, is an example of such a problem. The inability for classic computers to solve this problem in an efficient time scale is the key aspect which makes modern cryptography secure [8]. Additionally measurement instruments such as electron microscope and astronomic telescopes take advantage of quantum entanglement to increases the precision of their measurements consequentially. Insight into the coherence of quantum entanglement in the presence of static disorder will be significant to the development of these technologies.

[2]To whom correspondence should be addressed. E-mail: leo.thomas@mail.mcgill.ca

as the probability of the qubit being in one state grows to 100%, its probability of being in the opposite state decreases (to 0%). The probabilities oscillate in this way, such that their sum always equals 100%. We notice that the coupling energy affects the frequency of the qubit expectation value oscillations.

Although the expectation values only represent the probability of the qubit being found in a certain state, not much is lost by imagining the qubit as actually oscillating between these states. It may be easier to reason about the given results this way.

In order to derive the time evolution of the probability of finding the qubit in a given state we use a propagator known as the Green function, a fundamental solution to the Schrödinger equation:

$$G(E) = (E - \hat{H})^{-1}$$

Where $\hat{H}$ is the Hamiltonian operator representation of the system. The system may be a combination sub-systems, in which case the Hamiltonian is defined as the tensor product of the Hamiltonians of each sub-system:

$$\hat{H}_{AB} = \hat{H}_A \otimes \hat{H}_B$$

We take a Fourier transform of the Green function to move from an energy space to a time evolution:

$$G(t) = \int_{-\infty}^{+\infty} e^{-iEt}\, G(E)\, dE$$

Since G(t) is the time evolution of a fundamental solution to the Schrödinger equation, the basis vectors of G(t) are time dependent eigenstates, $|\psi(t)\rangle$. From these states we define the density matrix:

$$\rho = |\psi\rangle \langle\psi|$$

This gives us the time evolution of the expectation values of the state. If it is an entangled state, we use the partial trace operation to recover the dynamics specific to one element of the overall system.

$$\rho_A = tr_B(\rho_{AB})$$

Where ρ_{AB} is the density matrix of an entangled system, and where the diagonal elements of the reduced density matrix, ρ_A, are the time evolution of the expectation values of state A. (ie: $|\rho_{A_{ii}}|$ is the probability of finding the system A in state i, as a function of time)

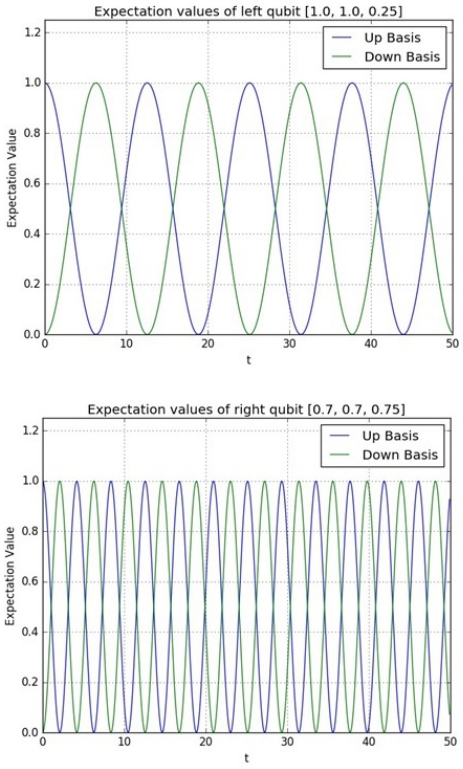

Fig. 1. Expectation values of qubits A ($\varepsilon_{up} = \varepsilon_{down} = 1.0, \tau = 0.25$, above) and B ($\varepsilon_{up} = \varepsilon_{down} = 0.7, \tau = 0.75$, below) oscillating independently

We deliberately chose unit-less quantities for the energies in each state, ε. According to the Plank-Einstein relation, $E = \hbar f$ where f has units of $\frac{1}{t}$, if our energy has units of $\hbar$, then t has units of $\frac{1}{E}$. This allows our method to be independent of scaling factors and our time evolution graphs throughout this paper to be valid for different definitions of energy.

Qubits coupled by an electrostatic force.

We begin by applying our method to a well know model, in order to calibrate the accuracy of our results. The model, represented graphically in figure 2, is of two qubits coupled with an electrostatic force. This energy affects the system when qubit A is the $|1\rangle$ state (down basis) and qubit B in the $|0\rangle$ state (up basis). This coupling has no time dependence.

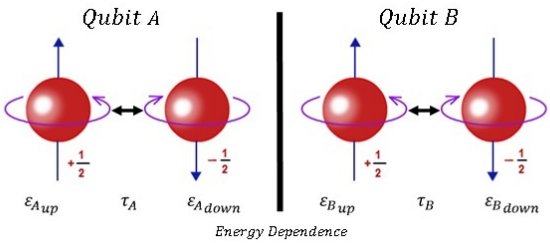

Fig. 2. A graphical representation of two qubits coupled with an electrostatic force

The Hamiltonian for this system is given by:

$$(\hat{H}_A \otimes \hat{H}_B) + U$$

Where $\hat{H}_A$ and $\hat{H}_B$ are of the following form (with different parameters):

$$\hat{H} = \begin{bmatrix} \varepsilon_{up} & \tau \\ \tau^* & \varepsilon_{down} \end{bmatrix}$$

Where U is the energy dependence term added to the combined Hamiltonian ($\hat{H}_{AB}$) at position (i,j), where

$$\hat{H}_{AB}(i,j) = \varepsilon_{A_{down}} + \varepsilon_{B_{up}}$$

In figure 3 we notice that as the probability oscillation of the qubits begin in phase the coupling energy has no dampening effect, since qubits A and B are in the same state at the same time. Because the qubits oscillate with different frequencies, their oscillations slowly come out of phase, and are antiphased sometime between $t = 20$ and $t = 25$. At this point we see the dampening effect of the coupling energy, since the qubits are more likely to be in opposite bases (A in state $|1\rangle$ and B in state $|0\rangle$) simultaneously during these times. We see this in the restriction of the expectation value oscillations to a maximally restricted state sometime between $t = 20$ and $t = 25$. We can interpret this as the coupling preventing the system from physically entering the above state. As their oscillation frequencies come back into phase, the dampening effect is lost and the qubits recover their original oscillation amplitudes.

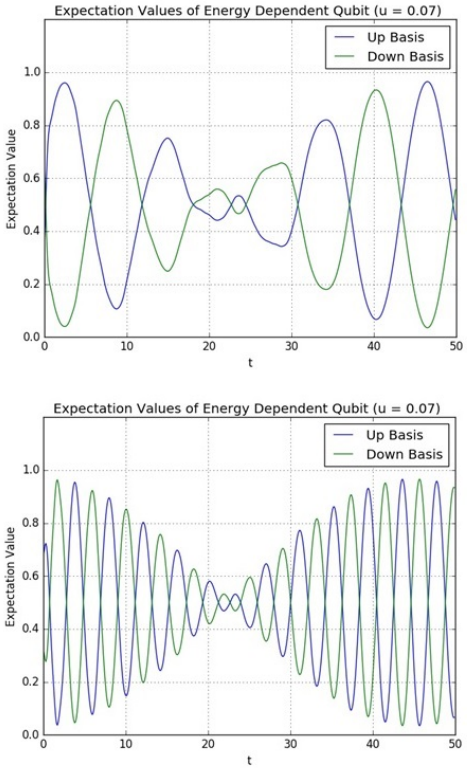

Fig. 3. Expectation values of qubits A and B oscillating with a coupling energy between states $\psi_A = |1\rangle$ and $\psi_B = |0\rangle$

These results are expected and documented [9], and confirm the accuracy of our method.

Qubits coupled to a dirty channel.

We now look at the objective model of the investigation, two qubits coupled to a quantum channel with variable levels of static disorder. Experimentally quantum particles must be entangled through some physical channel, such as a fiber optic cable or photon beam. This channel can, however, be modeled as a chain of uniformly coupled qubits, connected to each of the observed qubits at either end [10], as shown in figure 4. A small (≤ 30) chain of qubits can accurately model the behaviour of a quantum channel with an average fidelity of $\geq \frac{2}{3}$, that of a classic channel [11].

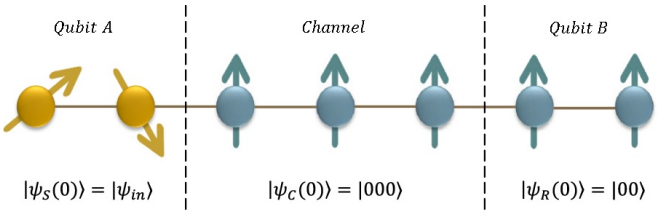

Fig. 4. Representation of two qubits entangled to a channel of length 3. Adapted from Rúben Sousa and Yasser Omar (2014) [12]

We use a chain of length six, (as opposed to a chain of length three, as shown in figure 4), where each qubit is coupled to the next by a constant energy of $\tau = 0.25$. Qubits A and B are coupled to the chain using the same method as described in the first part of the investigation, except the energy coupling terms are placed at the points of interaction between the qubits and each end of the chain, as opposed to the two qubits themselves.

The Hamiltonian of our combined system is:

$$\hat{H}_{AchB} = (\hat{H}_A \otimes \hat{H}_{Ch} \otimes \hat{H}_B) + U$$

The Hamiltonian of the channel is:

$$\hat{H}_{Ch} = \begin{bmatrix} \varepsilon_1 & \tau & 0 & 0 & \dots & 0 \\ \tau^* & \varepsilon_2 & \tau & 0 & \dots & 0 \\ 0 & \tau^* & \varepsilon_3 & \tau & \dots & 0 \\ \vdots & & & & \ddots & \vdots \\ 0 & . & . & . & \tau^* & \varepsilon_n \end{bmatrix}$$

The energy dependence terms, U are added to the Hamiltonian as the points (i,j), where each qubit interacts with either end of the channel where:

$$\hat{H}(i,j) = \varepsilon_{A_{down}} + \varepsilon_{Ch_1}$$

and

$$\hat{H}(i,j) = \varepsilon_{B_{up}} + \varepsilon_{Chn}$$

We introduce static disorder by randomizing the spin energies of the qubits in the chain ($\varepsilon_1 \dots \varepsilon n$). The level of disorder is defined by the range over which the chain's spin energies are uniformly distributed (ie: a distribution range of 0.2 results in energies being uniformly randomly distributed between -0.2 and 0.2).

We recover a graph of the time evolution of the expectation values of qubits A and B, and compare them to the original expectation values of those same qubits (shown in figure 1).

We take the average difference between the original and recovered expectation values, as a percentage, and plot these as a function of energy distribution range in figure 5.

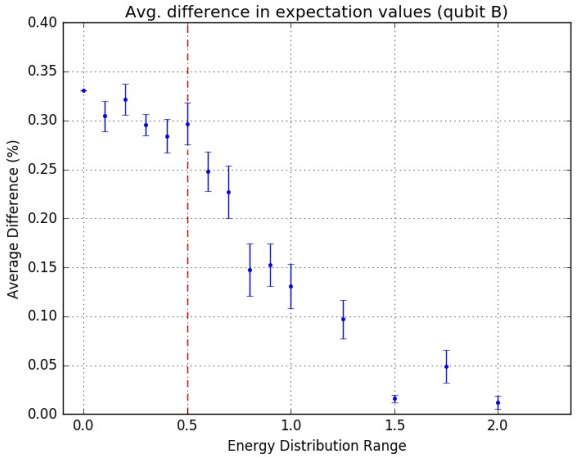

Fig. 5. Average difference in expectation values between entangled and non-entangled right qubits over $N = 31$ trials. Error-bars represent the variance of the mean of 31 trials for each energy distribution. Note a sharp drop-off around 0.5, the band width of the channel. As energies are distributed within a range smaller than the "width" of the channel, the channel is never fully blocked and the qubits remain somewhat entangled. Once the energy range allows for energies larger than the width of the channel a completely blocked channel occurs with increasing probability, returning a more and more isolated system.

In figure 5 we notice a sharp drop off in average difference between unentangled and entangled qubit expectation values after the channel's bandwidth (2τ, where τ is the coupling energy between each qubit in the chain, in this case, $\tau = 0.25$). We conclude that a highly disordered entanglement channel does not necessarily lead to qubit decoherence, if the channel is properly isolated from its environment, but rather leads to a perfectly isolated, or de-coupled system of two qubits. This result may have applications in experimental setting where separate qubits interfere destructively.

2. Conclusion

From this simulation we can conclude that the method described above leads to an accurate and insightful measurement of qubit dynamics for various quantum systems. We conclude that channels with high levels of static disorder act as barriers between qubits, effectively isolating the two systems. There is a sharp increase in the channels ability to isolate two qubits as the energy distribution allows for energies larger than the channel's bandwith.

Further steps include an experimental investigation to confirm the decoupling rates, as well as observing the quality of information transfer through these channels. This can be done by setting qubit A to a certain state at time t = 0, and calculating the probability of that state being correctly transferred to qubit B after a certain time, as a function of channel disorder.

A theoretical investigation may look at why entangled qubits experience a relatively constant average difference in expectation values as long as the chain remains open to some degree (differences within $\approx 5\%$ among energy distributions ranges 0.0 to 0.5, compared to $\approx 15\%$ among energy distribution ranges 0.5 to 1.0). Further theoretical investigation could attempt to derive a mathematical relationship between the energy distribution range and average difference of expectation values.

Ultimately the overarching goal and motivation of this investigation is to develop a correction scheme to decrease qubit decoupling and increase quality of information transfer in the presence of static disorder.

3. Acknowledgments

I would like to thank Dr. Michael Hilke for guidance in the theory, programming and analysis of the results throughout this investigation, and contribution to the contents of this paper. I would also like to thank Dr. Sabrina Leslie for guidance with regards the presentation of the results in this paper.

4. Appendix and commentary

All programming was done in Python (version 3.5), with SciPy (version 0.18) and Numpy (version 1.11) libraries, and ran on an Intel Core i7 processor.

Fourier Transform and Green's function. The numerical Fourier transform was approximated over an interval step of 0.001 and over an energy range of -5 to 5 (the energy range should cover a larger range than that of the eigenvalues of the Hamiltonian):

$$G(t) = \Delta E \sum_{n=-5}^{5} e^{-iEt}\, G(E)$$

where $\Delta E = 10^{-3}$

The Green's function, defined below for a single qubit, becomes unbounded as E approaches the eigenvalues of the Hamiltonian, (the matrix inverse operator requires a division by the determinant, which goes to 0 as E approaches the eigenvalues). While this is not a problem when symbolically integrating over G(E), this is an issue when numerically integrating, since the program needs to evaluate G(E) at each step. In order to mitigate this effect, we subtract a very small value of i from E, so that the real part of the determinant may go to zero, without the division by the determinant returning an error.

$$G'(E) = G(E - (i \times 10^{-8})) =$$
$$\begin{bmatrix} (E - (i \times 10^{-8})) - \varepsilon_{up} & -\tau \\ -\tau^* & (E - (i \times 10^{-8}))\varepsilon_{down} \end{bmatrix}^{-1}$$
$$= \begin{bmatrix} G'_{11}(E) & G'_{12}(E) \\ G'_{12}(E) & G'_{22}(E) \end{bmatrix}$$

Construction of the Hamiltonian. In order to construct the Hamiltonian of each combined system, we use the kronecker product function, also represented by the symbol $\otimes$, which multiplies two matrices as follows:

$$\begin{bmatrix} a_{11} & a_{12} \\ a_{11} & a_{22} \end{bmatrix} \otimes \begin{bmatrix} b_{11} & b_{12} \\ b_{11} & b_{22} \end{bmatrix} = \begin{bmatrix} a_{11}\begin{bmatrix} b_{11} & b_{12} \\ b_{11} & b_{22} \end{bmatrix} & a_{12}\begin{bmatrix} b_{11} & b_{12} \\ b_{11} & b_{22} \end{bmatrix} \\ a_{11}\begin{bmatrix} b_{11} & b_{12} \\ b_{11} & b_{22} \end{bmatrix} & a_{22}\begin{bmatrix} b_{11} & b_{12} \\ b_{11} & b_{22} \end{bmatrix} \end{bmatrix}$$

We combine Hamiltonians as follows:

$$\hat{H}_{ABC} = (\hat{H}_A \otimes \mathbb{I}_B \otimes \mathbb{I}_C) + (\mathbb{I}_A \otimes \hat{H}_B \otimes \mathbb{I}_C) + (\mathbb{I}_A \otimes \mathbb{I}_B \otimes \hat{H}_C)$$

Therefore the size of any combined Hamiltonian is the multiplicative sum of the sizes of its sub-systems.

Time complexity and Optimization. The Hamiltonian for our system of two qubits coupled to a chain of length n has size $2 \times n \times 2 = 4n$, which has $(4n)^2$ elements.

In order to find the time dependent Green's function, G(t), we must take the Fourier transform of each element of G(E), which has the same size as the Hamiltonian.

Calculating G(E) requires a matrix inverse at each step of E. Scipy's linalg.pinv() (a pseudo inverse function, which uses Gaussian elimination to solve for x where $xG(E) = \mathbb{I}$) was used, and is generally known to be an $O(N^3)$ operation, where N in the number of rows of $\hat{H}$. In our case $N = 4n$ with n being the chain length.

Time complexity of a program is often measured in FLOPS, the number of basic Floating Point OperationS necessary. Although our program operates on complex numbers, for which the basic operations are a bit more time consuming, an analysis using FLOPS may still provide a meaningful approximation of the program's time complexity.

Calculating a matrix inverse at each step of E, requires $(4n)^3$ operations per step, so $64 \times 10^4 n^3$ operations are needed to calculate G(E) from -5 to 5 with a step of $\Delta E = 0.001$. The CPU used to run these simulations can generally perform between 10×10^9 and 100×10^9 FLOPS per second (and slightly less for complex numbers).

We then take the Fourier transform of each element in G(E). Each transform has 10^4 steps with 5 FLOPS and one exponentiation by a 64 bit exponent, per step. Since we are numerically evaluating the Fourier transform, each evaluation is performed at a specific time value t, which ranges from 0 to 50 with a step of $\Delta t = 0.1$. This gives us a total of $(4n)^2 \times 10^4 \times 5 \times 64 \times 500 = 2.6 \times 10^{10} n^2$ FLOPS for the Fourier transform, and $6.4 \times 10^4 n^3$ FLOPS for calculating Green's energy function.

Once we have the time dependent Green's function, we perform a matrix multiplication to obtain the density matrix, ρ and two partial trace operation to retrieve the reduced density matrices for each of qubit A and B. These two operations, although complex, are only performed 500 times, on (relatively) small matrices, and therefore do not influence the time complexity noticeably.

The total time complexity, as a function of n, the length of the channel, is:

$$O(n) = 2.6 \times 10^{10} n^2 + 64 \times 10^4 n^3$$

This program's runtime scales polynomially as a function of channel length, but with massive constants. In practice, this program took about 2.5 minutes to retrieve the entangled expectation values of each qubit when connected to a chain of length 4, 4 minutes for a chain of length 5 and sometimes over 8 minutes for one of length 6.

Computations to optimize in this program are mostly related to the Fourier transform. The simple integration loop calculates G(E) at each step of E regardless of its value. If the value of G(E) changes very slightly over a certain range of E then the integration step can be increased in that range without noticeable loss of precision, reducing the number of steps over which it is necessary to integrate.

Another possible optimization would to suspend the evaluation of the Fourier transform, and then map the suspended function over each value of t, the desired time interval. This would allow for the use of much more precise timescales at a much lower run time.

5. References

1. Shor P (1995) Scheme for reducing decoherence in quantum computer memory. *Physical Review A* 52.
2. J. Hu, B. Yu MJLXSJGQGL (2015) Experimental quantum secure direct communication with single photons. *Light: Science and Applications*.
3. Thew NGR (2008) Quantum communication. *Nature Photonics* pp. 165–171.
4. Nicola J (2013) Computing: the quantum company. *Springer Nature* 498:286–288.
5. Dowling J, Milburn G (2003) Quantum technology: the second quantum revolution. *Philosophical Transactions of the Royal Society of London A: Mathematical, Physical and Engineering Sciences* 361:1655–1674.
6. C.-W. Chou, D.B. Hume JKDW, Rosenband T (2010) Frequency comparison of two high-accuracy al+ optical clocks. *Physical Review Letters*.
7. G. Vallone, D. Bacco DDSGVLGB, Viloresi P (2015) Experimental satellite quantum communications. *Physical Review Letters* 115.
8. Bennet C (1984) Quantum cryptography: Public key distribution and coin tossing. *International Conference on Computer Systems and Signal Processing* pp. 175–179.
9. Yu. A. Pashkin, T. Yamamoto OAYNDVAJST (2003) Quantum oscillations in two coupled charge qubits. *Nature* 421:823–826.
10. Bose S (2007) Quantum communication through spin chain dynamics: an introductory overview. *Contemporary Physics* 48(1):13–30.
11. Bose S (2003) Quantum communication through an unmodulated spin chain. *Physical Review Letters* 91(207901).
12. Sousa R, Omar Y (2014) Pretty good state transfer of entangled states through quantum spin chains. *New Journal of Physics* 16.